# The Lithosphere-Asthenosphere Boundary

Karen M. Fischer,[1] Heather A. Ford,[1] David L. Abt,[1] and Catherine A. Rychert[2]

[1]Department of Geological Sciences, Brown University, Providence, Rhode Island 02912; email: Karen_Fischer@brown.edu, Heather_Ford@brown.edu, abt.david.l@gmail.com

[2]Department of Earth Sciences, University of Bristol, Bristol BS8 1RJ, United Kingdom; email: glcar@bristol.ac.uk

Annu. Rev. Earth Planet. Sci. 2010. 38:551–75

First published online as a Review in Advance on March 4, 2010

The *Annual Review of Earth and Planetary Sciences* is online at earth.annualreviews.org

This article's doi: 10.1146/annurev-earth-040809-152438



0084-6597/10/0530-0551$20.00

## Key Words

plates, seismic properties, mantle rheology

## Abstract

Seismological models of upper-mantle structure are providing new constraints on the physical and chemical properties that differentiate the lithosphere from the asthenosphere. A wide variety of studies are consistent with an oceanic lithosphere that corresponds to a dry, chemically depleted layer over a hydrated, fertile asthenosphere. At the lithosphere-asthenosphere boundary beneath oceans and many Phanerozoic continental regions, observed seismic velocity gradients require a contrast in mantle hydration, fertility, and/or melt content, perhaps in combination with a vertical gradient in velocity anisotropy. Beneath cratons, evidence is growing for a deeper—but globally ubiquitous—asthenosphere. Some studies conclude that the cratonic lithosphere-asthenosphere boundary is gradual enough to be matched by a purely thermal gradient, whereas others indicate a more rapid transition and a contrast in composition or perhaps melt content.

## WHAT MAKES THE LITHOSPHERE PLATE-LIKE?

The concept of a strong lithosphere that translates as a relatively coherent layer over a weak asthenosphere (**Figure 1*a***) is fundamental to a modern understanding of plate motions, tectonics, and mantle convection. However, much remains to be learned about the physical and chemical properties that create the rheological differences between the lithosphere and asthenosphere.

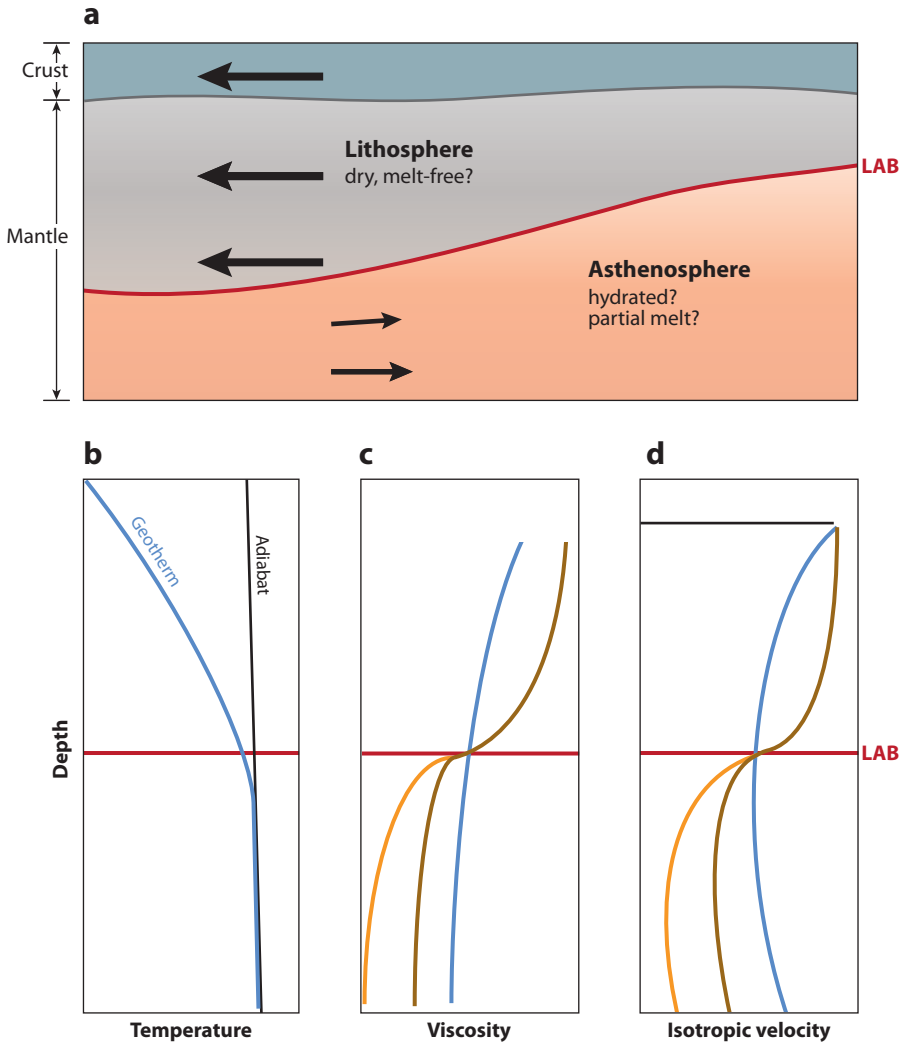


**Figure 1**

Schematic models of lithosphere-asthenosphere boundary (LAB) properties. (*a*) Depth profile through the lithosphere and asthenosphere. Arrows show the motion of a coherent lithospheric layer over a deforming asthenosphere. (*b*) Temperature as a function of depth. In the absence of other factors, the lithosphere would correspond to the cold thermal boundary layer represented by subadiabatic temperatures. (*c*) Mantle viscosity for three cases. Blue: the geotherm in panel *b*. Brown: the geotherm superimposed on a compositional difference at the LAB (dry lithosphere over hydrated asthenosphere). Orange: the latter case plus partial melt in the asthenosphere. (*d*) Isotropic shear velocity corresponding to the three cases in panel *c*. The black line schematically illustrates the velocity increase from the crust to the mantle.

Uncertainty surrounds even basic information such as the depth of the lithosphere-asthenosphere boundary (LAB), the magnitude of the rheological contrast between lithosphere and asthenosphere, and the depth range over which this contrast is distributed.

**LAB:** lithosphere-asthenosphere boundary

Colder temperatures at shallow depth in Earth undoubtedly play a role in making the lithosphere strong. A common definition of the lithosphere is that it represents the thermal boundary layer at Earth's surface where temperatures lie below the mantle adiabat defined by the potential temperature of the convecting mantle. A more precise definition is that the rigid lithosphere corresponds to the portion of the thermal boundary layer in which heat transport is purely conductive, and that the base of the thermal boundary layer represents a rheological boundary between the lithosphere and the convecting mantle (e.g., Sleep 2005) (**Figure 1*b***). Where mantle rocks are cold, their viscosity will be higher, producing higher viscosities within the lithosphere (**Figure 1*c***).



Other factors such as grain size, chemical composition, water content, and extent of partial melt affect viscosity. In particular, dehydration of mantle minerals as a result of melt extraction has been hypothesized as a source of increased viscosity in both oceanic (e.g., Hirth & Kohlstedt 1996, Karato & Jung 1998) and continental mantle lithosphere (e.g., Hirth et al. 2000, Lee et al. 2005, Sleep 2005, Lee 2006) (**Figure 1*c***). For example, Hirth & Kohlstedt (1996) proposed that the oceanic LAB is defined by a compositional boundary between hydrated, fertile peridotite in the asthenosphere and dry, chemically depleted peridotite in the lithosphere from which the oceanic crust was extracted by melting beneath mid-ocean ridges. In continental cratons, xenoliths indicate depleted mantle compositions to depths of roughly 200 km, leading to the hypothesis that the continents are underlain by high-viscosity mantle layers whose chemical buoyancy counteracts their cold temperatures (e.g., Jordan 1978, 1988; Boyd 1989; Griffin et al. 1999; Lee 2006), enabling the mantle layers to remain intact and attached to the overlying cratonic crust over billions of years (e.g., Pearson et al. 1995, Carlson et al. 1999, Shapiro et al. 1999). This chemically depleted layer was first described as the continental tectosphere with the assumption that chemical and thermal buoyancy were equal at all depths (Jordan 1978, 1988). More recently, differences in xenolith suites between low-temperature granular peridotites (which are highly melt-depleted) and high-temperature sheared peridotites (which are more fertile) have been used to argue that a chemically depleted, high-viscosity layer extends only to depths of 150–175 km, embedded in a thicker thermal boundary layer (Lee et al. 2005, Lee 2006) (**Figure 2**). In these latter models, dehydration of the chemically depleted layer is invoked as a means of increasing its viscosity (Lee et al. 2005, Lee 2006).

The presence of even a small amount of partial melt could significantly reduce mantle viscosity, especially if the melt is organized as aligned pockets at the grain scale or in shear zones at larger scales (e.g., Hirth & Kohlstedt 1995a,b; Mei et al. 2002; Takei 2002; Zimmerman & Kohlstedt 2004; Kohlstedt & Holtzman 2009; Takei & Holtzman 2009). Some studies have suggested that the asthenosphere contains a small amount of partial melt, either globally or at least on a widespread basis beneath oceans and continents (Anderson & Sammis 1970, Hirano et al. 2006, Mierdel et al. 2007). However, this topic is still the subject of considerable debate.

## GEOPHYSICAL SIGNATURES OF LITHOSPHERE-ASTHENOSPHERE BOUNDARY PROPERTIES

The thickness of the lithosphere and the rheological contrasts between the lithosphere and asthenosphere are expressed in a variety of geophysical observables, including seismic velocities, heat flow, electrical conductivity, and apparent elastic plate thickness. For example, off-axis of the East Pacific Rise, Baba et al. (2006) found a 60-km-thick layer of high-resistivity lithosphere

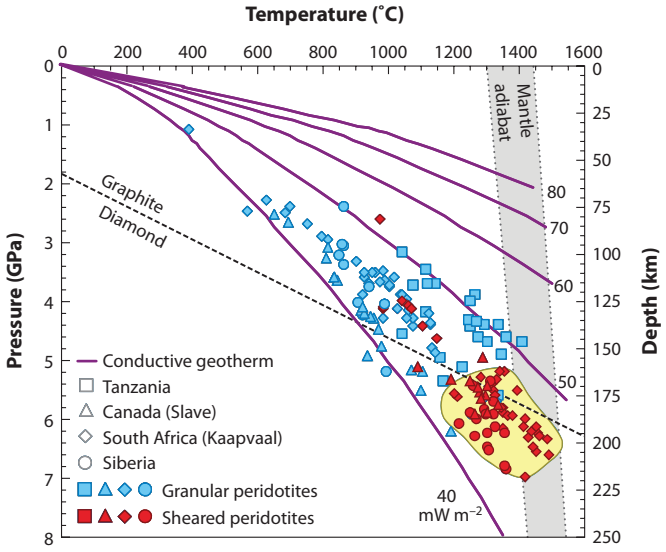


**Figure 2**

Xenolith thermobarometry data from different cratons combined with conductive geotherms inferred from surface heat flow. Blue symbols represent low-temperature granular peridotites; red symbols represent high-temperature sheared peridotites. The field of high-temperature sheared peridotites has been roughly outlined in yellow. Purple lines are conductive geotherms corresponding to different values of surface heat flow. Gray region outlines a range of mantle adiabats. From Lee (2006). Copyright 2006 American Geophysical Union. Reproduced/modified by permission of American Geophysical Union.

over more conductive asthenosphere. The lack of variation in the thickness of this layer (despite significant differences in plate age and cooling across the study region), coupled with anisotropy in asthenospheric conductivity, was interpreted as evidence that the mantle lithosphere corresponds to the layer that was depleted and dehydrated because of melting (Evans et al. 2005, Baba et al. 2006). Similarly, Hirth et al. (2000) concluded that both cratonic and ocean conductivity profiles were best explained by a dry lithosphere over a hydrated asthenosphere. Eaton et al. (2009) provide an excellent review of magnetotelluric studies and their implications for the LAB in cratons.

This paper focuses on the implications of seismological studies for models of the LAB. For purely thermal models, a gradual transition from cold lithosphere to warm asthenosphere produces a similarly gradual decrease in velocity (**Figure 1*d***) and an increase in attenuation unless another factor, such as olivine grain size in the mantle, is varied (Jackson et al. 2002, Faul & Jackson 2005). In mid-plate oceanic regions and beneath continents where mantle flow lacks a strong component of upwelling, temperature will increase over many tens of kilometers, and the vertical temperature gradient at any given depth is relatively small. For example, in numerical models that contain thick cratonic and thinner marginal lithosphere, if mantle viscosity depends on temperature but is not affected by composition or melt content, temperature rises gradually over the entire thickness of the lithosphere (Cooper et al. 2004) and temperature gradients are typically on the order of 5°C km$^{-1}$ (King & Ritsema 2000, Cooper et al. 2004). However, in some models where the thick, cratonic lithosphere is assumed to be of intrinsically higher viscosity than adjacent, thinner lithosphere, upwelling beneath regions of thin (~100-km) lithosphere produces temperature gradients of ~15°C km$^{-1}$ (Korenaga & Jordan 2002).

LAB velocity gradients can be distributed over a smaller depth interval if they are strongly influenced by a rapid vertical change in composition, such as the transition from a dry, depleted

lithosphere to a hydrated, fertile asthenosphere (**Figure 1*d***). The variation in shear velocity resulting from depletion effects is debated; it ranges from less than a percent (Schutt & Lesher 2006) to 2.5% (Lee 2003). The velocity variation associated with the degree of hydration strongly depends on the form of the volatiles—water in nominally anhydrous minerals such as olivine versus serpentine, for example—but the former case would typically be expected at asthenospheric temperatures. Direct experimental constraints on the effects of water in olivine at seismic frequencies are at an early stage (Aizawa et al. 2008). However, olivine rheology from creep experiments suggests that a sharp LAB dehydration boundary could produce a rapid (<10 km) and significant LAB velocity drop (Karato & Jung 1998, Karato 2004). Because water in olivine will also increase shear attenuation, reasonable limits on asthenospheric attenuation can be used to bound water effects on shear velocity. Based on typical asthenospheric attenuation values (Dalton & Ekström 2006), Rychert et al. (2007) indicate that the magnitude of this effect in shear velocity would be on the order of 4% or less.

**LPO:** lattice-preferred orientation

The presence of a small amount of partial melt in the asthenosphere could also dramatically reduce its shear velocity relative to a comparatively melt-free lithosphere, and the transition would be rapid if the LAB represented the mantle solidus or an abrupt change in permeability. Although the magnitude of the effect of melt on shear velocity strongly depends on the melt-distribution geometry (e.g., Hammond & Humphreys 2000, Takei 2002, Kawakatsu et al. 2009, Takei & Holtzman 2009), it is potentially very large (**Figure 1*d***). For example, a percent of partial melt could produce a velocity drop of 8% or more (Hammond & Humphreys 2000, Kawakatsu et al. 2009), although other models predict smaller velocity contrasts (Takei & Holtzman 2009).

Finally, because the LAB represents a reduction in viscosity with depth, the magnitude of strain related to present-day plate motion will increase below the boundary, likely producing lattice-preferred orientation (LPO) of olivine and orthopyroxene in the asthenosphere that reflects recent deformation. In contrast, the lower strain rates in the lithosphere would allow olivine and orthopyroxene LPO from past tectonic events to be preserved over longer timescales. Thus, in general, vertical variations in velocity anisotropy that reflect mantle LPO are expected across the LAB, and they could create sharp and significant mantle velocity gradients (e.g., Gaherty et al. 1999, Levin & Park 2000). Similarly, asthenospheric melt fabrics created by deformation would also produce anisotropy (Takei & Holtzman 2009) that could contrast with the lithosphere.

## SEISMOLOGICAL CONSTRAINTS ON THE LITHOSPHERE-ASTHENOSPHERE BOUNDARY

### Tools for Imaging the Lithosphere-Asthenosphere Boundary

A wide range of seismic phases and analysis methods can be used to constrain the depth of the LAB and its associated isotropic and/or anisotropic velocity gradients. Surface-wave tomography can provide robust constraints on three-dimensional, absolute shear-wave velocity structure at lithospheric and asthenospheric depths at both regional and global scales. Global surface-wave tomography (in some cases, including body-wave phases) has revealed systematic variations in apparent lithospheric thickness (defined as a lid of relatively fast velocities over a slower asthenospheric layer) between different tectonic environments (Cammarano & Romanowicz 2007, Kustowski et al. 2008, Lebedev & van der Hilst 2008, Nettles & Dziewonski 2008, Dalton et al. 2009, Romanowicz 2009). Similar results have been obtained in regional studies. In **Figure 3** the results of two different absolute shear-wave velocity models (Cammarano & Romanowicz 2007, Kustowski et al. 2008) indicate relatively thin lithosphere beneath young oceanic crust and much thicker and higher-velocity lithosphere beneath continental cratons. Definitions of LAB depth,

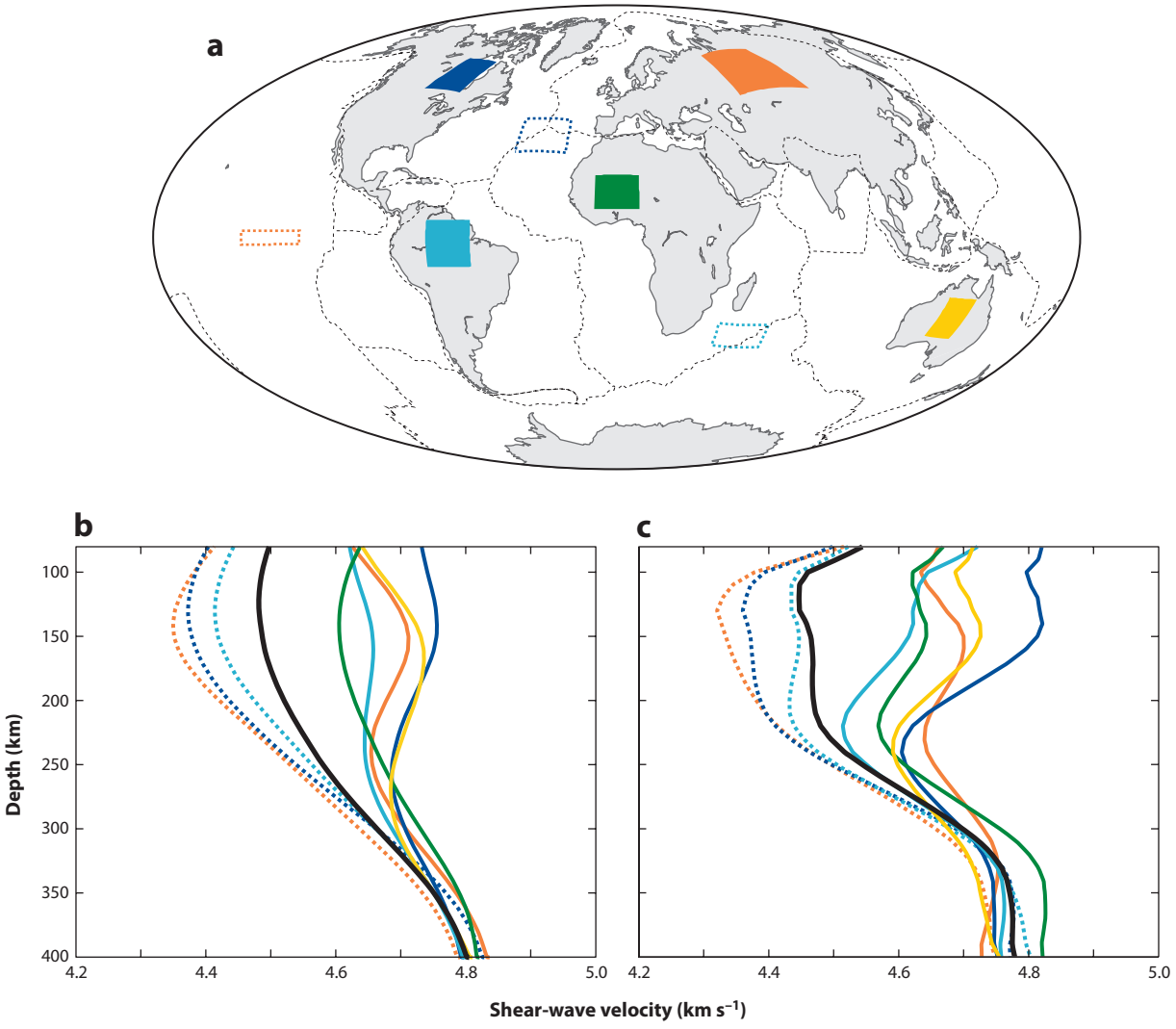


**Figure 3**

Shear velocity as a function of depth in the upper mantle from Cammarano & Romanowicz (2007) and Kustowski et al. (2008). (*a*) Regions sampled in the profiles are indicated by different colors for cratons (*solid blocks*) and oceans (*dashed lines*). (*b*) Shear velocity model of Kustowski et al. (2008). (*c*) Shear velocity model of Cammarano & Romanowicz (2007). The black lines in panels *b* and *c* indicate global averages of shear velocity. From Romanowicz (2009). Reprinted with permission from AAAS.

which often vary between surface-wave studies, include the depth of the maximum negative velocity gradient below the fast lid, the depth to a certain absolute velocity or velocity anomaly contour, and the depth where lateral velocity variations cease (see Eaton et al. 2009 for a detailed review). In addition, vertical variations in velocity anisotropy from surface-wave tomography have also been used to define the LAB, including changes in the strength and orientation of both radial and azimuthal anisotropy (Gaherty & Jordan 1995, Gaherty et al. 1999, Debayle & Kennett 2000, Simons et al. 2002, Gung et al. 2003, Gaherty 2004, Debayle et al. 2005, Sebai et al. 2006, Marone & Romanowicz 2007, Marone et al. 2007, Yuan & Romanowicz 2010). Global (e.g., Dalton et al.

2009) and regional (e.g., Yang et al. 2007) inversions of surface-wave data for attenuation structure are also beginning to yield constraints on LAB properties.

One limitation of surface-wave tomography is that surface waves alone cannot distinguish a change in mantle velocity that occurs instantaneously in depth from a change in velocity that occurs over tens of kilometers. For example, Eaton et al. (2009) showed that typical fundamental-mode surface data sets are equally well fit by a step-like drop in velocity at 160 km and a decrease in velocity of comparable amplitude that occurs from 125 to 225 km in depth. In addition, the starting model employed in the tomographic inversion will affect the final shear velocity model, as is evident in the profiles in **Figure 3** (Romanowicz 2009). Finally, whereas a low-velocity asthenospheric layer is widely observed beneath oceans and regions of relatively thin continental lithosphere, resolution of an asthenospheric layer beneath cratons is still debated (e.g., Gaherty & Jordan 1995, Gaherty et al. 1999, van der Lee 2002, Li & Burke 2006, Pedersen et al. 2009).

Body-wave tomography has also been used to estimate lithospheric thickness. However, with the relatively vertical direct-wave paths often used in regional body-wave tomography, lack of vertical resolution typically results in large uncertainties in LAB depth. In contrast, modeling of multiply reflected body-wave phases and triplicated arrivals yields robust constraints on the transition from fast lithospheric lid to low-velocity asthenosphere, although trade-offs between lid thickness and absolute velocity produce uncertainties on the order of 20 km in LAB depth (e.g., Grand & Helmberger 1984a,b; Tan & Helmberger 2007).

ScS reverberations that reflect off the LAB and arrivals such as Ps and Sp that convert at the LAB provide powerful complementary constraints on the depth of the LAB and its velocity gradient. All of these phases are primarily sensitive to changes in shear-wave structure (either shear-wave velocity or impedance). ScS reverberations from an LAB-like discontinuity have clearly been observed in oceanic regions (Revenaugh & Jordan 1991, Bagley & Revenaugh 2008), and numerous Ps and Sp studies have been used to infer LAB properties in both oceanic and continental regions (Sacks et al. 1979; Bostock 1998; Li et al. 2000; Collins et al. 2002; Oreshin et al. 2002; Li et al. 2004; Kumar et al. 2005a,b; Rychert et al. 2005, 2007; Vinnik et al. 2005; Chen et al. 2006; Mohsen et al. 2006; Sodoudi et al. 2006a,b; Wolbern et al. 2006; Hansen et al. 2007; Heit et al. 2007; Kumar et al. 2007; Li et al. 2007; Wittlinger & Farra 2007; Ozacar et al. 2008; Savage & Silver 2008; Snyder 2008; Chen 2009; Ford et al. 2009; Hansen et al. 2009; Kawakatsu et al. 2009; Rychert & Shearer 2009; Abt et al. 2010; Rychert et al. 2010). These phases provide better resolution of the LAB velocity gradient than is typical of surface-wave inversions alone. For example, incorporation of ScS reverberations with turning S waves and surface waves in the inversions of Gaherty et al. (1999) led to the conclusion that the LAB velocity gradient beneath old oceanic lithosphere occurs over 30 km or less. In another example, Rychert et al. (2007) inverted both Ps and Sp waveforms for LAB properties in eastern North America and found that the 5–8% velocity drop at the LAB occurs over 11 km or less. However, to use ScS reverberations and converted phases to infer the depths of mantle discontinuities, the data must be migrated to depth, which requires independent information on mantle structure above the discontinuity of interest. In addition, constraints on volumetric heterogeneity in the mantle are also helpful for interpreting apparent discontinuities. In many Sp and Ps studies, resulting discontinuities are compared with shear-wave velocity models from surface-wave tomography or some combination of surface-wave and body-wave tomography (e.g., Rychert et al. 2005, 2007; Savage & Silver 2008; Ford et al. 2009; Hansen et al. 2009; Rychert & Shearer 2009; Abt et al. 2010). Joint inversions—such as the inversion of ScS reverberations, turning S waves, and surface waves in Gaherty et al. (1999)—directly exploit the complementary information of the different data types.

Finally, discontinuities associated with a transition from a fast seismic lid to a deeper, slower, low-velocity zone have been observed at depths of 50 to 220 km by reflection and refraction

**Radial anisotropy:** a directional dependence in seismic wave velocity such that waves traveling in the horizontal plane with different vibration directions (horizontally versus vertically polarized) have different velocities

**Azimuthal anisotropy:** a directional dependence in seismic wave velocity such that waves propagating or vibrating at different azimuths in the horizontal plane have different velocities

**ScS:** a shear (S) body wave that reflects off the core-mantle boundary

**Ps:** a compressional (P) body wave that converts to an S wave at a discontinuity or rapid gradient in velocity

**Sp:** an S wave that converts to a P wave at a discontinuity or rapid gradient in velocity

experiments (Ryberg et al. 1996; MONA LISA Working Group 1997; Thybo & Perchuc 1997; Steer et al. 1998a,b; Morozova et al. 1999; Pavlenkova et al. 2002; Thybo 2006). Although more limited in geographic extent than is typical of passive-source studies, active-source methods offer higher spatial resolution of the details of lithospheric structure.

The interpretation of oceanic and continental LAB properties later in this paper focuses on a comparison of results from surface waves, ScS reverberation, converted phase (Sp and Ps) analyses, and multiply reflected S phases and triplicated arrivals. All these methods are primarily sensitive to shear-wave velocity structure, and surface-wave tomography typically has better vertical resolution than direct-phase body-wave tomography. Other constraints, such as active-source imaging, are also drawn into the discussion.

## Classic Mantle Discontinuities

A variety of classic mantle velocity discontinuities exist in the seismological literature, including the Gutenberg, Lehmann, and Hales discontinuities (Gutenberg 1948; Lehmann 1959, 1961; Hales 1969). Over time, these names have been assigned to discontinuities at a variety of depths, sometimes with positive or negative isotropic velocity contrasts and/or vertical variations in anisotropy. The original definition of the Hales discontinuity was as an increase in isotropic velocity with depth (Hales 1969). Since then it has commonly been interpreted as a discontinuity within the lithosphere (Revenaugh & Jordan 1991) sometimes associated with anisotropy (Fuchs 1983, Bostock 1998, Levin & Park 2000, Mercier et al. 2008). Some studies interpret the Gutenberg discontinuity as the base of the seismically fast lithospheric lid in oceanic regions and the Lehmann discontinuity as a boundary within the continental lithosphere (Revenaugh & Jordan 1991, Gaherty & Jordan 1995, Bostock 1998, Gaherty et al. 1999). Other studies attribute both the Lehmann and Gutenberg discontinuities to the LAB, with the latter representing a transition in anisotropy at the LAB beneath oceans and the former representing the transition at the LAB beneath continents (Gung et al. 2003). In the Preliminary Reference Earth Model, the Lehmann discontinuity was represented as the lower limit of a global low-velocity zone at a depth of 220 km (Dziewonski & Anderson 1981). For simplicity, the names of these classic discontinuities are not widely used in this paper.

## A Global View

Evidence is growing for a widespread, perhaps global, reduction in velocities at depths of 50 to 130 km. Thybo & Perchuc (1997) introduced the idea of the 8° discontinuity, a low-velocity layer (both P and S velocity) in the continental lithosphere with its top at a depth of ~100 km. Thybo (2006) contains an excellent review of the presence of this feature in long-range, active-source seismic profiles. A significant body of Sp and Ps receiver-function studies have found evidence for discontinuities characterized by a significant negative velocity contrast in the depth range of 50 to 130 km. These studies span oceanic regions (Li et al. 2000, Collins et al. 2002, Li et al. 2004, Kumar et al. 2005a, Vinnik et al. 2005, Wolbern et al. 2006, Heit et al. 2007, Kumar et al. 2007, Kawakatsu et al. 2009, Rychert & Shearer 2009), regions of relatively thin (<130 km) continental lithosphere (Oreshin et al. 2002; Kumar et al. 2005b; Rychert et al. 2005, 2007; Angus et al. 2006; Chen et al. 2006; Mohsen et al. 2006; Sodoudi et al. 2006a,b; Hansen et al. 2007; Heit et al. 2007; Kumar et al. 2007; Li et al. 2007; Ozacar et al. 2008; Chen 2009; Ford et al. 2009; Rychert & Shearer 2009; Abt et al. 2010; Rychert et al. 2010), and continental regions with thicker cratonic-style lithosphere (Ford et al. 2009, Rychert & Shearer 2009, Abt et al. 2010, Rychert et al. 2010). For example, Rychert & Shearer (2009) carried out a global study of Ps receiver functions

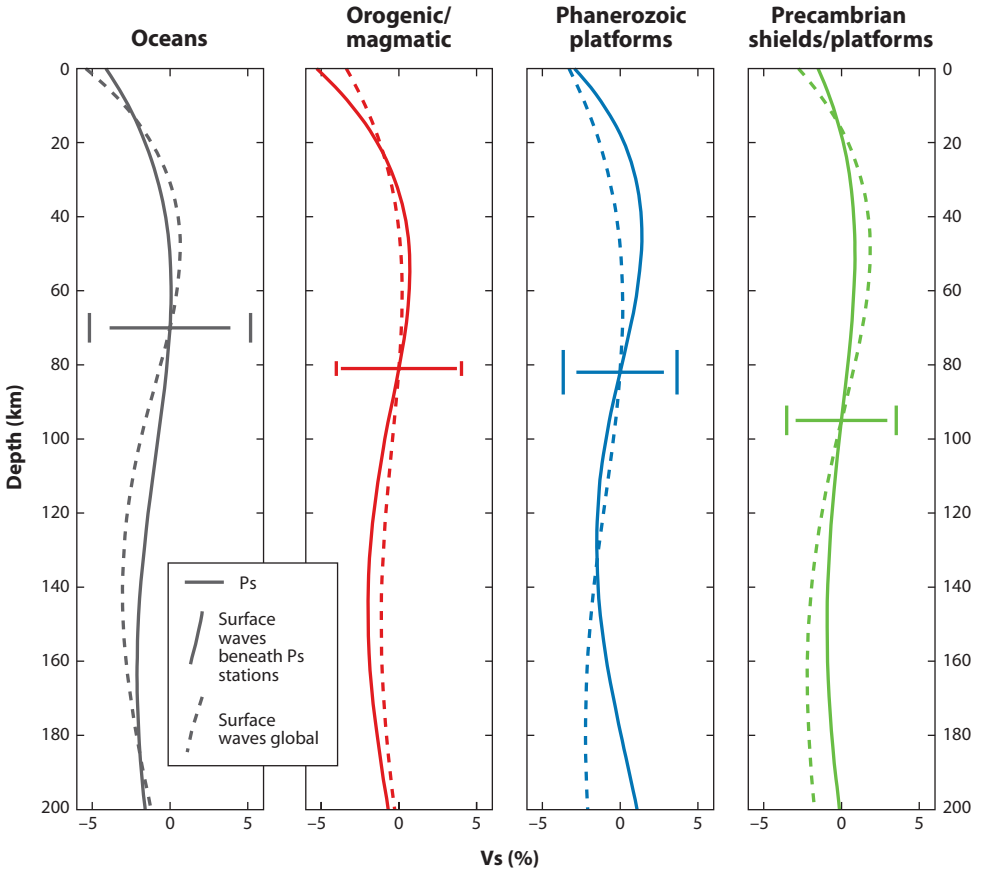


**Figure 4**

Comparison of LAB properties [depth and velocity drop (percent Vs)] from Ps receiver functions (Rychert & Shearer 2009) with a global Vs model from surface-wave tomography (Nettles & Dziewonski 2008) for four types of tectonic regions. Surface-wave results are shown both as averages for the tectonic regions from the entire global model (*dashed lines*) and beneath the stations with Ps receiver-function results (*solid curved lines*). Ps results are shown as tectonic region averages by horizontal lines. Short vertical lines are standard errors in Ps depths. Separation between horizontal lines and vertical bars indicates uncertainty in the LAB velocity drop. Vs percentages are calculated with respect to the average surface-wave Vs at the Ps conversion depth in each region. From Rychert & Shearer (2009). Reprinted with permission from AAAS.

and found a shear velocity drop at an average depth of 70 ± 4 km beneath oceans, 81 ± 2 km beneath Phanerozoic orogens and magmatic belts, and 95 ± 4 km beneath Precambrian shields and platforms (**Figure 4**).

The widespread prevalence of a negative discontinuity in the 50–130-km depth range might be taken as evidence for a global discontinuity with a single origin, such as a global LAB. In fact, when Rychert & Shearer (2009) compared their average Ps negative-discontinuity depths with average absolute shear-wave velocity profiles for the same tectonic regions, the discontinuities appeared to fall within the transition from the maximum shear-wave velocity (which presumably lies within the lithosphere) to the minimum shear-wave velocity (which should lie within the asthenosphere). Based on this comparison of averaged results, it might be tempting to interpret

all of these discontinuity sightings as the LAB. However, this interpretation would be a mistake because a number of the negative discontinuities found by Rychert & Shearer (2009) and at similar depths in other studies (Ford et al. 2009, Abt et al. 2010) lie in cratonic regions where surface-wave tomography near the station clearly shows a fast lithospheric layer that extends to depths of 150 km or more (**Figure 5**). At these stations, the negative discontinuity lies within the lithosphere and cannot be interpreted as the LAB. Rather, it represents an intralithospheric reduction in velocity, similar to the dip in absolute shear velocity at depths of approximately 100 km seen in the cratonic profiles from the surface-wave tomography model of Cammarano & Romanowicz (2007) (**Figure 3*c***). Further evidence for this line of reasoning comes from cratonic xenolith data. The idea of an LAB at depths of roughly 100 km in cratons is incompatible with the xenolith evidence that a layer of cold, depleted mantle extending to at least 150 km (**Figure 2**) has remained coupled to the overlying crust for billions of years (Jordan 1978, 1988; Boyd 1989; Pearson et al. 1995; Carlson et al. 1999; Griffin et al. 1999; Lee 2006).

Sp receiver-function results from station ULM (part of the Canadian National Seismic Network) in the Canadian shield provide a good example of a cratonic station with a negative discontinuity internal to the lithosphere (**Figures 5** and **6**) (Abt et al. 2010). At ULM, Sp receiver functions contain a negative arrival that corresponds to a drop in velocity at a depth of 101 ± 14 km (**Figure 6*d*,*e***). Absolute shear-wave velocity from surface-wave tomography beneath ULM indicates fast lithospheric velocities to at least 150 km and a gradual gradient to a minimum asthenospheric velocity at 220 km (**Figure 6*f***). Thus, the potential LAB depth range lies between 220 km and 150 km, indicating that the negative Sp arrival corresponds to a conversion from a negative discontinuity within the lithosphere. In contrast, at station VTV (part of the Caltech Regional Seismic Network) near the San Andreas Fault in southern California, a strong negative Sp phase (**Figure 6*a*,*b***) falls within the transition from asthenosphere to lithosphere in absolute shear velocity (120-km to 45-km depth), indicating that this discontinuity can be interpreted as the LAB.

In addition to the negative discontinuities at depths of 50–130 km described above, Ps and Sp studies have also found negative discontinuities in the 130–300-km depth range, sometimes interpreting them as the LAB (Sacks et al. 1979; Kumar et al. 2005b, 2006, 2007; Mohsen et al. 2006; Sodoudi et al. 2006a; Heit et al. 2007; Wittlinger & Farra 2007; Snyder 2008; Hansen et al. 2009) and sometimes not (Bostock 1998, Savage & Silver 2008). Rychert et al. (2010) contains a comprehensive review of both Ps and Sp studies, including ones not referenced here that modeled phases with anisotropic discontinuities that are not obviously negative in an isotropic sense.

A global map of Sp studies that found a negative phase at depths of less than 300 km and interpreted it as the LAB is shown in **Figure 7**. Sp receiver functions are sometimes considered a more reliable indicator of mantle discontinuities from the Moho to depths of roughly 300 km because Ps receiver functions contain reverberations from crustal reverberations that may

**Figure 5**

Mantle-discontinuity depths estimated from Sp receiver functions in North America by Abt et al. (2010) (*a*) and in Australia by Ford et al. (2009) (*b*). The dots, colored for discontinuity depth, represent Sp piercing points that have been interpolated onto a fine grid and smoothed with a circular filter with a 30-km radius. (*a*) North America. Black inverted triangles indicate stations where the negative Sp phase is interpreted as the lithosphere-asthenosphere boundary (LAB), white inverted triangles are stations where the phase is interpreted as a mid-lithospheric discontinuity (MLD), and gray stations indicate ambiguity in the interpretation of the negative Sp phase. (*b*) Australia. Negative Sp phases at stations in Phanerozoic eastern Australia (COEN and stations to its east) and at two sites just within the eastern margin of the Proterozoic craton (BBOO and STKA) are interpreted as the LAB. Negative Sp phases at most stations in the Proterozoic and Archean craton (WRAB and the stations to its west) are interpreted as mid-lithospheric discontinuities.

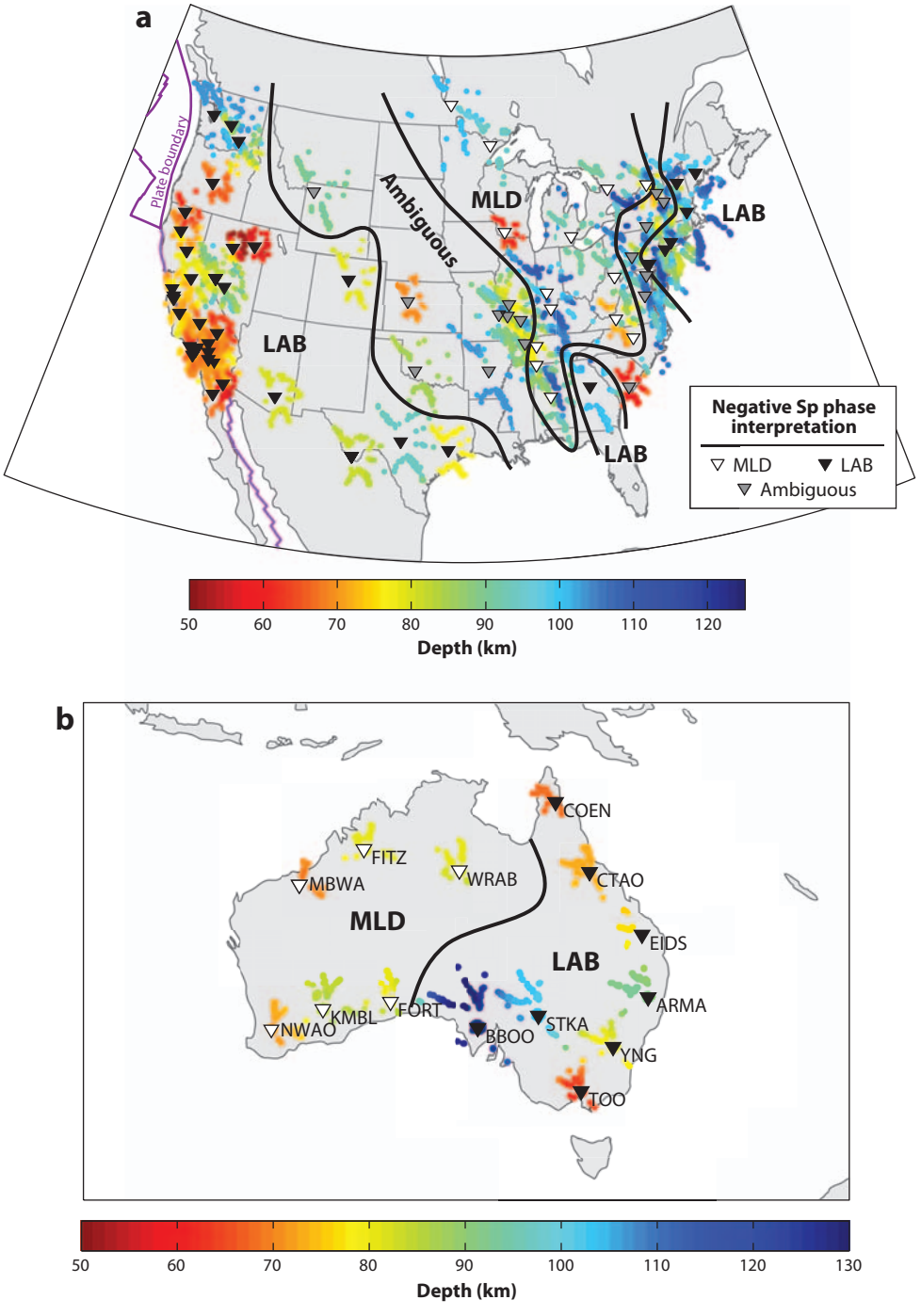

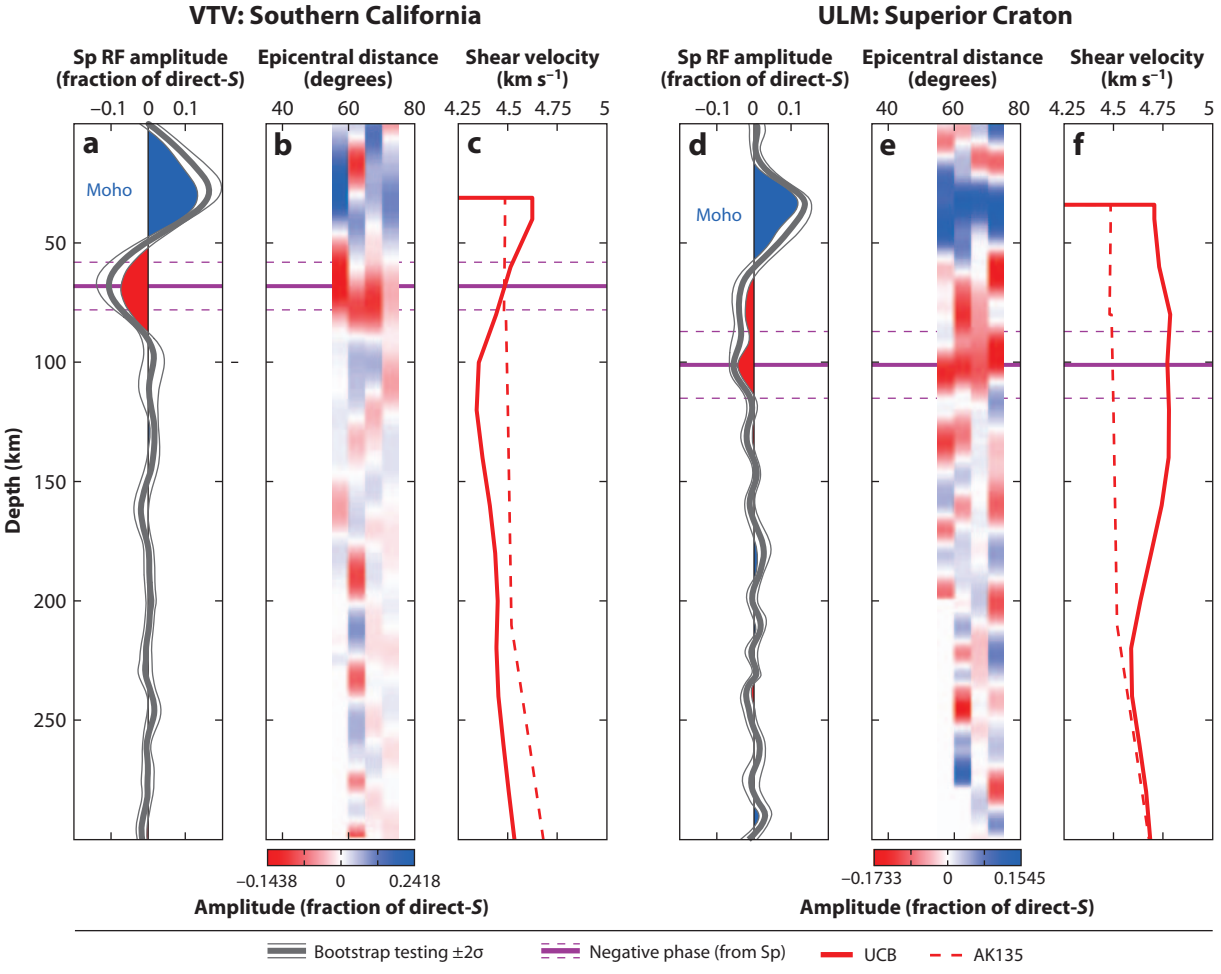


**Figure 6**

Sp receiver functions and absolute shear-wave velocity profiles at two stations in North America from Abt et al. (2010): VTV in southern California (*a–c*) and ULM in the Superior Craton in Canada (*d–f*). (*a*, *d*) Mean single-station receiver functions (RFs) from bootstrap testing (thick gray lines) $\pm 2\sigma$ (thin gray lines). (*b*, *e*) Sp receiver functions binned by epicentral distance (not bootstrapped). Blue indicates positive amplitude (a velocity increase with increasing depth) and red indicates negative amplitude (a velocity decrease with increasing depth). In panels *a* and *d*, the portions colored red and blue represent the minimum amplitude of the receiver function, accounting for the $2\sigma$ uncertainties. The large positive phase corresponds to the crust-mantle boundary (the Moho or Mohorovičić discontinuity). The most prominent negative phase following the Moho is marked with the magenta line, and $2\sigma$ errors are given by the dashed magenta lines. (*c*, *f*) Thick red line shows mantle shear-velocity profiles at VTV and ULM averaged from a 3D surface-wave model, from a University of California, Berkeley (UCB) study by Yuan & Romanowicz (2010). Dashed red line shows the AK135 velocity model (Kennett et al. 1995) for reference.

overprint mantle signals. However, when care is taken to interpret Ps phases only when they appear to be unbiased from crustal phases (e.g., Rychert & Shearer 2009), robust constraints on LAB and intralithospheric discontinuities may be obtained. For example, of the 21 stations where a negative discontinuity was identified from both Ps data (Rychert & Shearer 2009) and Sp data (Ford et al. 2009, Abt et al. 2010), 14 of the depths estimated from the Ps analysis fall within the Sp depth error bars and 19 fall within 10 km of the Sp error bars.

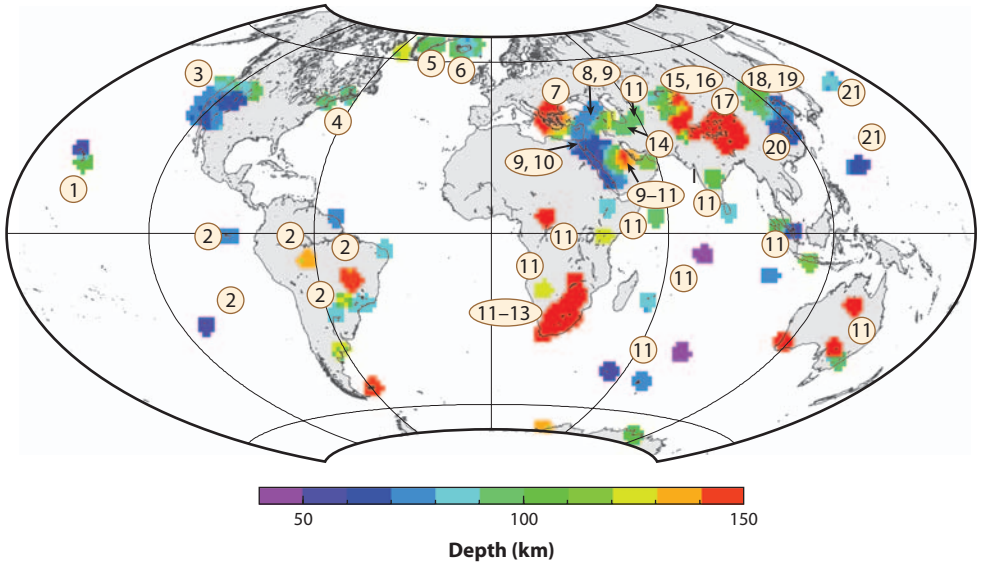


**Figure 7**

Compilation of Sp studies that interpret a negative phase as the LAB. Colored backgrounds correspond to the depths reported by the numbered studies. Whereas the color scale ends at a depth of 150 km, some studies see Sp arrivals and interpret them as the LAB at depths of as much as 300 km. 1: Li et al. (2004). 2: Heit et al. (2007). 3: Li et al. (2007). 4: Rychert et al. (2007). 5: Kumar et al. (2005a). 6: Vinnik et al. (2005). 7: Sodoudi et al. (2006a). 8: Angus et al. (2006). 9: Mohsen et al. (2006). 10: Hansen et al. (2007). 11: Kumar et al. (2007). 12: Wittlinger & Farra (2007). 13: Hansen et al. (2009). 14: Sodoudi et al. (2009). 15: Kumar et al. (2005b). 16: Oreshin et al. (2002). 17: Kumar et al. (2006). 18: Chen et al. (2008). 19: Chen (2009). 20: Sodoudi et al. (2006b). 21: Kawakatsu et al. (2009).

## The Oceanic Lithosphere-Asthenosphere Boundary

The oceanic lithosphere provides a well-controlled environment in which to test competing models for the origin of the LAB. Because plate age and cooling increase systematically from mid-ocean ridges, models in which the lithosphere-to-asthenosphere transition is primarily controlled by temperature would predict an increase in LAB depth with plate age. In contrast, if the oceanic lithosphere represents a layer of dry and depleted mantle created by melt extraction at the ridge, its thickness would not be expected to appreciably change as a function of plate age. In addition, an LAB that reflects only temperature would appear as a velocity drop distributed over tens of kilometers. Gradients in mantle water or melt content could be similarly gradual. However, if the chemical boundary between the lithosphere and the more hydrated, fertile asthenosphere represents the peridotite solidus, it would likely have been created as a relatively sharp discontinuity (**Figure 1*d***). Furthermore, even accounting for the diffusion of hydrogen in olivine, its width would increase by less than 5 km over a typical 150-Ma lifespan for oceanic lithosphere (Hirth & Kohlstedt 1996). If the LAB velocity gradient is too large to be explained by contrasts in depletion and hydration, it could represent a transition from a melt-free lithosphere to an asthenosphere that contains partial melt (**Figure 1*d***); in this case, the LAB could correspond to either the peridotite solidus or a boundary in permeability.

Surface-wave inversions in oceanic regions typically show an increase in the apparent thickness of the oceanic lithosphere as defined by fast isotropic velocities with plate age (Nishimura & Forsyth 1989, Nettles & Dziewonski 2008) (**Figure 8*b,d***). Alone, this result could be taken as

**Figure 8**

Global shear-wave velocity structure from surface-wave tomography. (*a*) Map view showing location of depth profile in panels *b* and *c* (*red line*). (*b*) Isotropic shear-wave velocity structure in profile. (*c*) Radial anisotropy in profile. (*d*, *e*) Averages from global model for oceanic regions with different plate ages, with isotropic velocities (*d*) and radial anisotropy (*e*). From Nettles & Dziewonski (2008). Copyright 2008 American Geophysical Union. Reproduced/modified by permission of American Geophysical Union.

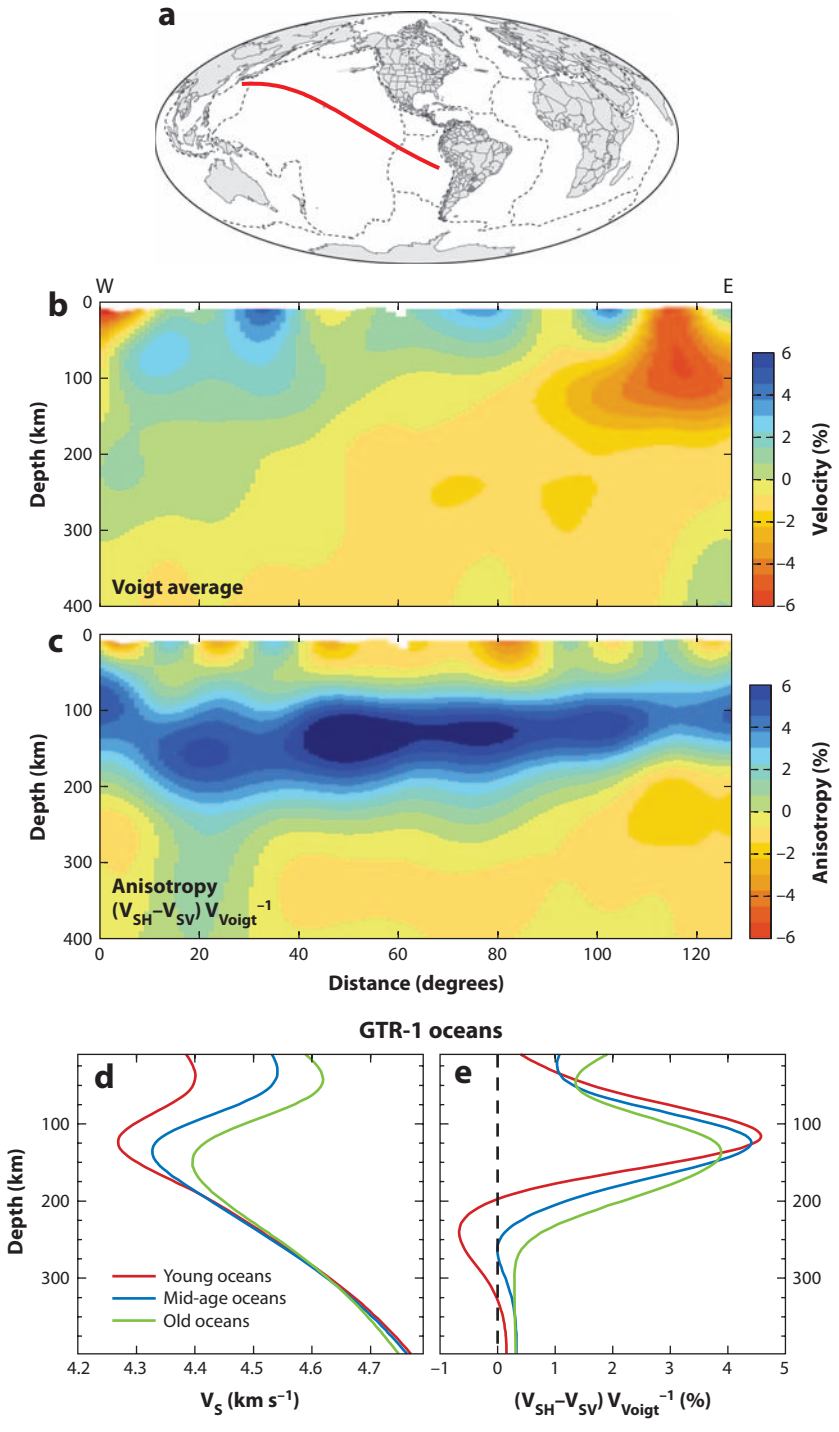

evidence that the thickness of the oceanic lithosphere is largely controlled by a cooling geotherm. However, when radial anisotropy is considered, a different picture emerges in which wave velocities for SH motion (horizontal vibration normal to the wave path) are systematically higher than velocities for SV motion (vibration polarized in the vertical plane containing the path) in a layer at depths of ~80–220 km (Ekström & Dziewonski 1998, Gung et al. 2003, Nettles & Dziewonski 2008) (**Figure 8*c*,*e***). This geometry of anisotropy would be developed if olivine a-axes were systematically aligned by strain in this layer and then sampled over a wide range of azimuths by the surface waves used in the inversion. The top of this layer beneath the Pacific lies at depths of 80–100 km (Nettles & Dziewonski 2008) (**Figure 8*c***), suggesting a relatively uniform-thickness lithosphere over a deforming asthenosphere, even beneath the East Pacific Rise where plate-cooling models predict a lithosphere of negligible thickness.

Waveform modeling of multiply bouncing S phases and triplicated arrivals (Tan & Helmberger 2007) considered together with inversion of surface waves, turning S waves, and ScS reverberations (Gaherty et al. 1999) also argue for a lack of age dependence in the thickness of the oceanic lithosphere. The latter study samples old oceanic lithosphere from Tonga to Hawaii and the former study samples lithosphere with a younger average age from Tonga to southern California, yet both found fast seismic lids with a thickness of approximately 60 km. In addition, the ScS reverberations in Gaherty et al. (1999) indicate that the negative velocity gradient at 60 km along the older path must occur over 30 km or less. More recent analysis of ScS reverberations on a wide variety of paths from Hawaii to circum-Pacific stations yielded fast-lid thicknesses of 72 km to 108 or 112 km. Although some of this variation appears to be significant at the 95% confidence level, no clear correlation of lid thickness and average lithospheric age exists. Modeling indicated that the transition from lid to low-velocity layer on these paths also occurs over 30 km or less.

Sp and Ps studies have also sampled the oceanic lithosphere. Reported depths of negative discontinuities at and near oceanic islands are highly variable, ranging from 40 km to 140 km (Li et al. 2000, Collins et al. 2002, Li et al. 2004, Kumar et al. 2005a, Vinnik et al. 2005, Wolbern et al. 2006, Heit et al. 2007, Kumar et al. 2007, Rychert & Shearer 2009). A significant amount of this variability is not correlated with plate age. For example, among Sp measurements at island stations in the Pacific (**Figure 7**), LAB depth estimates are 50–60 km at Kauai and 100–110 km at Hawaii, both on middle-aged oceanic lithosphere (Li et al. 2004), and 70 km beneath the Galapagos and 50 km at Easter Island, both on younger oceanic lithosphere (Heit et al. 2007). At island stations where Rychert & Shearer (2009) analyzed Ps receiver functions, LAB depth estimates at individual stations vary from 48 km to 98 km about the oceanic mean of 70 $\pm$ 4 km, and again do not correlate with plate age. However, because the lithosphere beneath ocean island stations may have been perturbed by hotspot-related processes, these locations are not ideal to test for an age-dependent trend in lithospheric thickness.

In contrast, Kawakatsu et al. (2009) analyzed Ps and Sp receiver functions at borehole stations on relatively unperturbed oceanic lithosphere and did observe a correlation between LAB depth and plate age. In the Philippine Sea Plate, 25 Ma–old lithosphere appeared to be 55 km thick, and 49 Ma–old lithosphere was 76 $\pm$ 1.8 km. In the Pacific Plate, receiver functions were noisier, but 129 Ma–old lithosphere yielded a thickness of 82 $\pm$ 4.4 km, a value that matches the apparent thickness of the plate subducting beneath Japan. Kawakatsu et al. (2009) conclude that these LAB depths can be modeled with a cooling-plate model in which the asymptotic plate thickness is 104 km and the temperature at the base of the plate is 1358°C.

The existence of Sp and Ps phases from an oceanic LAB argues that the LAB velocity gradient is relatively sharp, although waveform modeling at the particular Sp and Ps frequencies employed in each study is necessary to accurately bound the velocity drop and depth range. For example, the waveform modeling by Kawakatsu et al. (2009) indicated a velocity drop of 7–8% over less

than 10–15 km, which they attributed to horizontal melt-rich layers in the asthenosphere. Other modeling at oceanic stations obtained velocity drops of 10–20%, assuming a velocity change that is a step function in depth (Li et al. 2000, Collins et al. 2002). However, even in the absence of direct modeling of a particular data set, approximate bounds on LAB velocity gradients may be inferred from other modeling studies. If a velocity drop occurs as a step function in depth and the amplitude of the resulting Sp phase is *A*, then if the same drop in velocity occurs over a depth range of *H*, where the incident wavelength of the S phase at the discontinuity is 1/2 *H*, the Sp amplitude will be ~70% of *A*; as *H* increases further with respect to wavelength, Sp amplitude will continue to decrease (Rychert et al. 2007, 2010). [Rychert et al. (2010) figure 3 illustrates this effect and is a corrected version of Rychert et al. (2007) figure 7.] Assuming a 7% velocity drop at the oceanic LAB (Gaherty et al. 1999), a roughly 10-s Sp period, and typical signal-to-noise levels, velocity gradients distributed over 30 km or less should produce clear Sp phases, but Sp amplitudes from gradients over 40 km or more will be difficult to observe. The smaller periods often used in Ps studies result in still tighter constraints.

To summarize, radial anisotropy in surface-wave tomography (Ekström & Dziewonski 1998, Gung et al. 2003, Nettles & Dziewonski 2008), the relatively constant fast seismic lid thickness beneath the Pacific (Gaherty et al. 1999, Tan & Helmberger 2007), and the lack of age dependence in the depth of the base of the lid from ScS reverberations (Bagley & Revenaugh 2008) are all consistent with a model in which the oceanic lithosphere corresponds to a dry, chemically depleted layer over a hydrated, fertile, and possibly partially molten asthenosphere. This model also explains the constant depth to the top of the high-conductivity layer observed near the East Pacific Rise (Evans et al. 2005, Baba et al. 2006). Assuming this model, the apparent increase in depth of a fast layer of isotropic velocities away from ridges (**Figure 8*b,d***) and the deepening of the lower boundary of the radially anisotropic layer (**Figure 8*c,e***) could represent gradual cooling of the oceanic mantle below the base of the compositionally defined oceanic lithosphere. In contrast, Kawakatsu et al. (2009) interpret the correlation of plate age and apparent LAB depth at the boundary of the Pacific and Philippine Sea plates as an example of plate thickness controlled by cooling temperatures alone, although they invoke melt below the LAB to produce the observed Sp and Ps phases. However, the apparent LAB seen in this study could correspond to a dehydrated lithosphere that varies in thickness. In yet another alternative, the discontinuity at 55-km depth for 25 Ma in Kawakatsu et al. (2009) could correspond to the base of a compositionally defined lithosphere, whereas the greater discontinuity depths at larger ages could represent the growth of a thermal boundary layer beyond the base of the dehydrated layer. In this latter case, the absence of converted phases from the base of the dehydrated layer at older ages might be explained by a decrease in the impact of water on olivine rheology and mantle shear velocity as temperatures cool (Faul & Jackson 2005; G. Hirth, personal communication).

Regardless of the factors that control the thickness of the oceanic lithosphere, the relatively rapid velocity gradients required at its base by ScS reverberations and Sp and Ps receiver functions indicate that the LAB cannot be explained by thermal gradients alone. Some studies have concluded that temperature, or a combination of temperature and grain size, can largely explain the shear-velocity structure of the oceanic upper mantle imaged by surface waves (e.g., Faul & Jackson 2005, Stixrude & Lithgow-Bertelloni 2005, Priestley & McKenzie 2006). However, whereas the relatively gradual velocity gradients predicted for old oceanic geotherms can match much of the broad LAB velocity gradient typical of surface-wave models, they fail to predict the LAB velocity gradients of 5% or more over depth ranges of 30 km or less indicated by ScS reverberations and converted phases. Thus, a contrast in hydration, fertility, and/or melt is required at the LAB. Vertical differences in anisotropy or grain size across the LAB may contribute to observed velocity gradients, but creating a contrast in viscosity sharp enough to produce a sufficiently

rapid anisotropic gradient would still require a variation in water or melt content at the LAB. Furthermore, Behn et al. (2009) conclude on the basis of grain size modeling that the oceanic asthenosphere must be hydrated for asthenospheric anisotropy to exist.

## The Phanerozoic Continental Lithosphere-Asthenosphere Boundary

In continental regions, the longer, more complex, and less well-understood thermal history of the lithosphere does not predict a simple correlation of lithospheric age and thickness. However, the LAB velocity gradient is still a useful diagnostic of whether the LAB may be explained by purely thermal models versus a contrast in composition or melt content, although some assumptions about mantle flow are typically required. For example, in models where mantle flow does not contain a strong upwelling component and mantle viscosity is not affected by a variation in composition or melt content, positive temperature gradients will in general be distributed from shallow depths in the lithosphere into the asthenosphere. In models appropriate for many Phanerozoic continental regions, where a decrease in lithospheric thickness from the craton to the origin drives moderate small-scale convection, temperature gradients at LAB depths are typically on the order of 5°C $km^{-1}$ (King & Ritsema 2000, Cooper et al. 2004). In some models, upwelling beneath regions of thin (~100-km) lithosphere produces temperature gradients of ~15°C $km^{-1}$ (Korenaga & Jordan 2002), but in these cases the gradient still occurs over many tens of kilometers (more than 50–70 km). This type of thermal structure, on its own, would not be capable of generating a clear Sp or Ps arrival at a distinct depth (Ford et al. 2009). In regions of active upwelling or complicated flow, more localized LAB thermal gradients cannot be ruled out.

Numerous studies of Sp (**Figures 5** and **7**) and Ps receiver functions provide evidence for a relatively sharp and isolated LAB velocity gradient in Phanerozoic continental regions (Oreshin et al. 2002; Kumar et al. 2005b; Rychert et al. 2005, 2007; Chen et al. 2006; Mohsen et al. 2006; Sodoudi et al. 2006a,b; Hansen et al. 2007; Heit et al. 2007; Kumar et al. 2007; Li et al. 2007; Ozacar et al. 2008; Chen 2009; Ford et al. 2009; Rychert & Shearer 2009; Abt et al. 2010; Rychert et al. 2010). In the northeastern United States, where the lithosphere has not experienced significant tectonic activity since the early Mesozoic, Rychert et al. (2007) jointly modeled Sp and Ps arrivals and determined that the LAB velocity drop was 5–10% over 5–11 km at depths of 87–105 km. Using the relationship of shear-wave velocity to temperature developed by Faul & Jackson (2005) based on experimental data, thermal gradients exceeding 20°C $km^{-1}$ are required to explain the observed velocity gradients, and they must be concentrated in a layer less than 11 km thick. This result is clearly incompatible with the gradual thermal gradients expected for this type of tectonic environment (e.g., King & Ritsema 2000, Korenaga & Jordan 2002, Cooper et al. 2004). However, the gradient can be matched with a contrast in chemical depletion and hydration across the LAB or with the presence of a small fraction of partial melt in the asthenosphere, both possibly in combination with vertical variations in anisotropy. Analysis of data at a larger number of North American stations revealed that similar Sp arrivals exist widely in the Phanerozoic eastern United States (Abt et al. 2010), although they are interpretable as the LAB only in certain areas. [Thick lithosphere appears to extend from the craton across portions of the Appalachians (**Figure 5**). At these stations, the observed Sp phase is best interpreted as an intralithospheric discontinuity; in some cases, it is left uninterpreted.] Strong Sp arrivals have also been documented in Phanerozoic regions of eastern Australia (Kumar et al. 2007, Ford et al. 2009) (**Figure 5**). For the 10–11-s Sp dominant periods in Ford et al. (2009), typical velocity gradients in eastern Australia range from a 5% drop over 0 km to a 10% drop over 30 km or less. Gradients over more than 40 km can be ruled out based on the Sp modeling in Australia, if velocity drops are limited to no more than 10%, a value greater than the isotropic shear-velocity drop from lithosphere to asthenosphere seen in

surface wave models (Gaherty et al. 1999, Nettles & Dziewonski 2008, Romanowicz 2009, Yuan & Romanowicz 2010). Although Sp phases alone do not constrain the depth range of the LAB velocity gradient as tightly as when they are combined with Ps, an LAB gradient that is confined to no more than 30 km in depth is still too localized to be matched by typical thermal models. The widespread observation of distinct Sp and Ps phases from potential LAB depths in Phanerozoic continental regions suggests that a relatively sharp velocity gradient (<30 km) is a common feature of thinner (<130-km) lithosphere.

Some of the largest-amplitude Sp phases from LAB depths occur in the tectonically active western United States (Li et al. 2007, Abt et al. 2010) (**Figure 5**). For example, at station VTV in southern California, a strong negative Sp arrival and a slow asthenospheric low-velocity zone are observed (**Figure 6**). Compared with LAB Sp arrivals in the eastern United States, LAB phase amplitudes in the western United States are systematically larger, indicating a greater LAB velocity gradient (Abt et al. 2010). This observation is consistent with surface-wave and body-wave tomography that indicate unusually slow velocities in the asthenosphere of the western United States (Grand 1994, Humphreys & Dueker 1994, van der Lee & Nolet 1997, van der Lee 2002, Godey et al. 2004, Marone et al. 2007, Li et al. 2008, Nettles & Dziewonski 2008, Roth et al. 2008, Yuan & Romanowicz 2010). The large amplitudes of these phases suggest that the asthenosphere contains partial melt on a widespread basis, consistent with recent and active magmatism in the region. However, detailed modeling of actual LAB velocity gradients is required to verify this hypothesis relative to the possibility that the asthenosphere is hydrated. Finally, very steep LAB temperature gradients resulting from small-scale convection and strong localized upwelling may play a significant role at some stations, although it seems unlikely that this type of asthenospheric flow would be consistent enough to ubiquitously explain strong LAB velocity gradients.

## The Cratonic Lithosphere-Asthenosphere Boundary

Thick layers of isotropically fast velocity are a common feature of cratonic lithosphere (e.g., **Figure 3**), and recently global correlations of shear velocity and shear attenuation have provided supporting evidence for a chemically distinct layer at depths of less than 225 km in continents (compared with depths of less than 125 km beneath oceans) (Dalton et al. 2009). Several surface-wave inversions have also shown that even the thickest continental lithosphere is underlain by a layer of radial anisotropy with the same geometry that is observed in the shallower layer of radial anisotropy observed in the oceanic asthenosphere (SH fast versus SV) (Gung et al. 2003, Marone et al. 2007, Nettles & Dziewonski 2008). This result suggests that an asthenospheric shear zone persists beneath cratons. (These studies also show that the shallow cratonic lithosphere is radially anisotropic, but this anisotropy is typically interpreted as fossil fabric created by Proterozoic or Archean deformation.) Some studies also indicate a transition in the direction of azimuthal anisotropy across the cratonic LAB (Debayle & Kennett 2000, Simons et al. 2002, Sebai et al. 2006, Marone & Romanowicz 2007, Yuan & Romanowicz 2010) or a transition from radial anisotropy in the lithosphere to azimuthal anisotropy in the asthenosphere (Gaherty 2004). However, Debayle et al. (2005) suggest that Australia is the only continent beneath which azimuthal anisotropy indicates asthenospheric flow parallel to plate motion.

Whereas the above studies are broadly consistent with the presence of an asthenospheric shear zone beneath cratons, the sharpness of the velocity gradient beneath cratons is more ambiguous. Studies that observe a deep (>150-km) negative Sp or Ps phase and interpret it as the LAB include work done in the Kalahari Craton (Kumar et al. 2007, Wittlinger & Farra 2007, Hansen et al. 2009), the Slave Craton (Snyder 2008), the Baltic Shield (Sacks et al. 1979), Australia (Kumar et al. 2007), and the Arabian Shield (Mohsen et al. 2006, Hansen et al. 2007). In contrast,

other studies find no evidence for negative discontinuities at these depths in the Superior Craton and Proterozoic terranes of the central United States (Abt et al. 2010; also see station ULM in **Figure 6**) or in Australia (Ford et al. 2009). Authors of yet other studies observe a deep phase but do not interpret it as the LAB (Savage & Silver 2008).

The situation beneath the Kalahari Craton is particularly confusing. Savage & Silver (2008) and Hansen et al. (2009) observe Sp phases at comparable depths (150 km and 160 km) but interpret them differently—as a discontinuity internal to the lithosphere versus the LAB, respectively. A discontinuity in this depth range would correspond to the base of the most chemically depleted layer indicated by xenoliths (**Figure 2**; also see Lee 2006). However, Kumar et al. (2007) and Wittlinger & Farra (2007) argue for negative LAB Sp phases at 200–300 km and 300 km, respectively. The two sets of Sp receiver functions bear little resemblance to each other and are not easily reconciled.

In Australia, Kumar et al. (2007) and Ford et al. (2009) analyzed Sp receiver functions at three common cratonic stations (WRAB, NWAO, and STKA). However, whereas Kumar et al. (2007) observed the largest negative Sp arrivals at depths of 164, 180, and 207 km, Ford et al. (2009) saw no significant negative Sp phases at these depths but instead observed clear negative Sp arrivals at depths of 72 $\pm$ 9 km, 81 $\pm$ 14 km, and 104 $\pm$ 9 km. Ford et al. (2009) obtained similar results at other cratonic stations and interpreted all but two of the cratonic Sp phases as the top of an intralithospheric, low-velocity zone (**Figure 5*b***). (The two exceptions were at stations STKA and BBOO, located near the eastern margin of the craton, whose Sp phases followed trends observed in Phanerozoic eastern Australia.) Abt et al. (2010) found a comparable intralithospheric discontinuity in the North American craton at depths of 60–115 km (**Figure 5*a***). The origin of this feature is uncertain. It might be a relict of cratonic mantle formation, such as the base of an original dehydrated, depleted lithospheric layer below which the thicker cratonic lithosphere grew (Yuan & Romanowicz 2010). Alternatively, it could reflect alteration of the cratonic lithosphere by melt migration and metasomatism; for example, it might be the top of a melt cumulate layer.

An absence of significant converted phases from the base of the cratonic lithosphere would indicate that the LAB velocity gradient is gradual. For example, the results of Ford et al. (2009) in the Australian craton and Abt et al. (2010) in the North American craton are consistent with LAB velocity gradients that are distributed over more than 70 km in depth, and thus they may be explained by an LAB that is controlled by temperature alone. In this case, the properties that govern the LAB in cratons could fundamentally differ from those in more recently deformed continental terranes and oceans. However, if strong converted phases at periods of $\sim$10 s or less are generated at the cratonic LAB, then the asthenosphere could be hydrated or contain partial melt on a global basis. If LAB phases were observed in some cratonic regions but not others, it would be reasonable to conclude that cratonic LAB properties were simply variable. However, the lack of agreement among studies at overlapping stations indicates that further work is required to resolve this issue. A careful analysis of the dominant periods used in each study and their respective constraints on LAB velocity gradients would be especially helpful.

## CONCLUSIONS

A variety of seismic studies indicate a seismically fast oceanic lithosphere of roughly constant thickness above a layer of radial anisotropy. These results, together with the conductivity structure near the East Pacific Rise, favor a model in which the oceanic lithosphere corresponds to a dry, chemically depleted layer over a hydrated, fertile asthenosphere. At the boundary of the Pacific and Philippine Sea plates, apparent LAB depth correlates with plate age and has been interpreted as evidence for thermal control of oceanic-lithospheric thickness, but these results do not preclude

the presence of a compositionally distinct oceanic lithosphere. Regardless of the processes that control lithospheric thickness, the relatively steep velocity gradients required at the base of the lithosphere by ScS reverberations and Sp and Ps receiver functions (<30 km in depth) indicate that the LAB cannot be explained by thermal gradients alone. Rather, a contrast in mantle hydration, fertility, and/or melt is required at the LAB, perhaps in combination with a vertical gradient in velocity anisotropy.

In many Phanerozoic continental regions, Sp and Ps receiver functions require LAB velocity gradients that occur over 30 km or less (in some cases, less than 15 km). Where likely mantle-flow fields lack complexity and strong upwelling, these LAB velocity gradients are too large and localized in depth to be matched by models without a contrast in hydration, fertility, and/or melt at the LAB.

Beneath cratons, the persistence of radial anisotropy at depths below the LAB and rotation of azimuthal anisotropy across the LAB argue for a global asthenosphere. Sp and Ps analyses reach divergent conclusions on the sharpness of subcratonic LAB velocity gradients. In some studies, no converted phases were observed at potential LAB depths, arguing for a gradual LAB velocity gradient that could be explained by a purely thermal variation from lithosphere to asthenosphere. Other studies obtained significant converted phases in the LAB depth range, suggesting sharper velocity gradients and possibly contrasts in composition or melt content at the cratonic LAB.

## DISCLOSURE STATEMENT

The authors are not aware of any affiliations, memberships, funding, or financial holdings that might be perceived as affecting the objectivity of this review.

## ACKNOWLEDGMENTS

This research was supported by the U.S. National Science Foundation under awards EAR-0538155 and EAR-0641772.

## LITERATURE CITED

Abt DL, Fischer KM, French SW, Ford HA, Yuan H, Romanowicz B. 2010. North American lithospheric discontinuity structure imaged by Ps and Sp receiver functions. *J. Geophys. Res.* Submitted

Aizawa Y, Barnhoorn A, Faul UH, FitzGerald JD, Jackson I, et al. 2008. Seismic properties of Anita Bay Dunite: an exploratory study of the influence of water. *J. Petrol.* 49(4):841–54

Anderson DL, Sammis C. 1970. Partial melting in the upper mantle. *Phys. Earth Planet. Inter.* 3:41–50

Angus DA, Wilson DC, Sandvol E, Ni JF. 2006. Lithospheric structure of the Arabian and Eurasian collision zone in eastern Turkey from S-wave receiver functions. *Geophys. J. Int.* 166:1335–46

Baba K, Chave AD, Evans RL, Hirth G, Mackie RL. 2006. Mantle dynamics beneath the East Pacific Rise at 17°S: insights from the Mantle Electromagnetic and Tomography (MELT) experiment. *J. Geophys. Res.* 111:B02101

Bagley B, Revenaugh J. 2008. Upper mantle seismic shear discontinuities of the Pacific. *J. Geophys. Res.* 113:B12301

Behn MD, Hirth G, Elsenbeck JR. 2009. Implications of grain-size evolution on the seismic structure of the oceanic upper mantle. *Earth Planet. Sci Lett.* 282:178–89

Bostock MG. 1998. Mantle stratigraphy and evolution of the Slave province. *J. Geophys. Res.* 103(B9):21183–200

Boyd FR. 1989. Compositional distinction between oceanic and cratonic lithosphere. *Earth Planet. Sci. Lett.* 96:15–26

Cammarano F, Romanowicz B. 2007. Insights into the nature of the transition zone from physically constrained inversion of long-period seismic data. *Proc. Natl. Acad. Sci. USA* 104:9139–44

Carlson RW, Pearson DG, Boyd FR, Shirey SB, Irvine G, et al. 1999. Re-Os systematics of lithospheric peridotites: implications for lithosphere formation and preservation. In *Proceedings of the 7th International Kimberlite Conference, J.B. Dawson Volume*, ed. JJ Gurney, JL Gurney, MD Pascoe, SR Richardson, pp. 99–108. Rondebosch, South Africa: Dep. Geol. Sci., Univ. Cape Town

Chen L. 2009. Lithospheric structure variations between the eastern and central North China Craton from S- and P-receiver function migration. *Phys. Earth Planet. Inter.* 173:216–27

Chen L, Tao W, Zhao L, Zheng TY. 2008. Distinct lateral variation of lithospheric thickness in the northeastern North China Craton. *Earth Planet. Sci. Lett.* 267:56–68

Chen L, Zheng TY, Xu WW. 2006. A thinned lithospheric image of the Tanlu Fault Zone, eastern China: constructed from wave equation based receiver function migration. *J. Geophys. Res.* 111:B09312

Collins JA, Vernon FL, Orcutt JA, Stephen RA. 2002. Upper mantle structure beneath the Hawaiian swell: constraints from the ocean seismic network pilot experiment. *Geophys. Res. Lett.* 29(11):1522

Cooper CM, Lenardic A, Moresi L. 2004. The thermal structure of stable continental lithosphere within a dynamic mantle. *Earth Planet. Sci. Lett.* 222:807–17

Dalton CA, Ekström G. 2006. Global models of surface wave attenuation. *J. Geophys. Res.* 111:B05317

Dalton CA, Ekström G, Dziewonski AM. 2009. Global seismological shear velocity and attenuation: a comparison with experimental observations. *Earth Planet. Sci. Lett.* 284:65–75

Debayle E, Kennett B, Priestley K. 2005. Global azimuthal seismic anisotropy and the unique plate-motion deformation of Australia. *Nature* 433:509–12

Debayle E, Kennett BLN. 2000. Anisotropy in the Australasian upper mantle from Love and Rayleigh waveform inversion. *Earth Planet. Sci. Lett.* 184:339–51

Dziewonski A, Anderson DL. 1981. Preliminary reference earth model. *Phys. Earth Planet. Inter.* 25:297–356

Eaton DW, Darbyshire F, Evans RL, Grutter H, Jones AG, Yuan X. 2009. The elusive lithosphere-asthenosphere boundary (LAB) beneath cratons. *Lithos* 109:1–22

Ekström G, Dziewonski AM. 1998. The unique anisotropy of the Pacific upper mantle. *Nature* 394:168–72

Evans RL, Hirth G, Baba K, Forsyth D, Chave A, Mackie R. 2005. Geophysical evidence from the MELT area for compositional controls on oceanic plates. *Nature* 437:249–52

Faul UH, Jackson I. 2005. The seismological signature of temperature and grain size variations in the upper mantle. *Earth Planet. Sci. Lett.* 234(1–2):119–34

Ford HA, Fischer KM, Abt DL, Elkins-Tanton LT, Rychert CA. 2009. The lithosphere-asthenosphere boundary beneath Australia imaged by Sp phases. *Eos Trans. AGU* 90(52), Fall Meet. Suppl., Abstr. DI11A-05

Fuchs K. 1983. Recently formed elastic anisotropy and petrological models for the continental subcrustal lithosphere in southern Germany. *Phys. Earth Planet. Inter.* 31:93–118

Gaherty JB. 2004. A surface wave analysis of seismic anisotropy beneath eastern North America. *Geophys. J. Int.* 158:1053–66

Gaherty JB, Jordan TH. 1995. Lehmann discontinuity as the base of an anisotropic layer beneath continents. *Science* 26:1468–71

Gaherty JB, Kato M, Jordan TH. 1999. Seismological structure of the upper mantle: a regional comparison of seismic layering. *Phys. Earth Planet. Inter.* 110:21–41

Godey S, Deschamps F, Trampert J, Snieder R. 2004. Thermal and compositional anomalies beneath the North American continent. *J. Geophys. Res.* 109:B01308

Grand SP. 1994. Mantle shear structure beneath the Americas and surrounding oceans. *J. Geophys. Res.* 99(B6):11591–621

Grand SP, Helmberger DV. 1984a. Upper mantle shear structure beneath the North Atlantic Ocean. *J. Geophys. Res.* 89:11465–75

Grand SP, Helmberger DV. 1984b. Upper mantle shear structure of North America. *Geophys. J. R. Astron. Soc.* 76:399–438

Griffin WL, O'Reilly SY, Ryan CG. 1999. The composition and origin of sub-continental lithospheric mantle. In *Mantle Petrology: Field Observations and High Pressure Experimentation: A Tribute to Francis R. (Joe) Boyd*, ed. Y Fei, CM Bertka, BO Mysen, pp. 13–45. St. Louis, MO: Geochem. Soc.

Gung YC, Panning M, Romanowicz B. 2003. Global anisotropy and the thickness of continents. *Nature* 422:707–11

Gutenberg B. 1948. On the layer of relatively low wave velocity at a depth of about 80 kilometers. *Bull. Seismol. Soc. Am.* 38:121–48

Hales AL. 1969. A seismic discontinuity in the lithosphere. *Earth Planet. Sci. Lett.* 7:44–46

Hammond WC, Humphreys ED. 2000. Upper mantle seismic wave velocity: effects of realistic partial melt geometries. *J. Geophys. Res.* 105(B5):10975–86

Hansen SE, Nyblade AA, Julià J, Dirks PHGM, Durrheim RJ. 2009. Upper-mantle low-velocity zone structure beneath the Kaapvaal craton from *S*-wave receiver functions. *Geophys. J. Int.* 178:1021–27

Hansen SE, Rodgers AJ, Schwartz SY, Al-Amri AMS. 2007. Imaging ruptured lithosphere beneath the Red Sea and Arabian Peninsula. *Earth Planet. Sci. Lett.* 259:256–65

Heit B, Sodoudi F, Yuan X, Bianchi M, Kind R. 2007. An S receiver function analysis of the lithospheric structure in South America. *Geophys. Res. Lett.* 34:L14307

Hirano N, Takahashi E, Yamamoto J, Abe N, Ingle SP, et al. 2006. Volcanism in response to plate flexure. *Science* 313:1426–28

Hirth G, Evans RL, Chave AD. 2000. Comparison of continental and oceanic mantle electrical conductivity: Is the Archean lithosphere dry? *Geochem. Geophys. Geosyst.* 1(12):1030

Hirth G, Kohlstedt DL. 1995a. Experimental constraints on the dynamics of the partially molten upper mantle: deformation in the diffusion creep regime. *J. Geophys. Res.* 100(B2):1981–2001

Hirth G, Kohlstedt DL. 1995b. Experimental constraints on the dynamics of the partially molten upper mantle: 2. Deformation in the dislocation creep regime. *J. Geophys. Res.* 100(B8):15441–49

Hirth G, Kohlstedt DL. 1996. Water in the oceanic upper mantle: implications for rheology, melt extraction and the evolution of the lithosphere. *Earth Planet. Sci. Lett.* 144:93–108

Humphreys ED, Dueker KG. 1994. Physical state of the western U.S. upper mantle. *J. Geophys. Res.* 99:9635–50

Jackson I, Fitz Gerald JD, Faul UH, Tan BH. 2002. Grain-size-sensitive seismic wave attenuation in polycrystalline olivine. *J. Geophys. Res.* 107(B12):2360

Jordan TH. 1978. Composition and development of the continental tectosphere. *Nature* 274:544–48

Jordan TH. 1988. Structure and formation of the continental tectosphere. *J. Petrol. Spec. Lithosphere Issue*, pp. 11–37

Karato S. 2004. Mapping water content in the upper mantle. In *Inside the Subduction Factory*, ed. J Eiler, *Geophys. Monogr. Ser.* 138:135–52. Washington, DC: AGU

Karato S, Jung H. 1998. Water, partial melting and the origin of the seismic low velocity and high attenuation zone in the upper mantle. *Earth Planet. Sci. Lett.* 157:193–207

Kawakatsu H, Kumar P, Takei Y, Shinohara M, Kanazawa T, et al. 2009. Seismic evidence for sharp lithosphere-asthenosphere boundaries of oceanic plates. *Science* 324:499–502

Kennett BLN, Engdahl ER, Buland R. 1995. Constraints on seismic velocities in the Earth from traveltimes. *Geophys. J. Int.* 122:108–24

King SD, Ritsema J. 2000. African hot spot volcanism: small-scale convection in the upper mantle beneath cratons. *Science* 290:1137–40

Kohlstedt DL, Holtzman BK. 2009. Shearing melt out of the Earth: an experimentalist's perspective on the influence of deformation on melt extraction. *Annu. Rev. Earth Planet. Sci.* 37:561–93

Korenaga J, Jordan TH. 2002. On the state of sublithospheric upper mantle beneath a supercontinent. *Geophys. J. Int.* 149:179–89

Kumar P, Kind R, Hanka W, Wylegalla K, Reigber Ch, et al. 2005a. The lithosphere-asthenosphere boundary in the North-West Atlantic region. *Earth Planet. Sci. Lett.* 236:249–57

Kumar P, Yuan X, Kind R, Kosarev G. 2005b. The lithosphere-asthenosphere boundary in the Tien Shan-Karakoram region from S receiver functions: evidence for continental subduction. *Geophys. Res. Lett.* 32:L07305

Kumar P, Yuan XH, Kind R, Ni J. 2006. Imaging the colliding Indian and Asian lithospheric plates beneath Tibet. *J. Geophys. Res.* 111:B06308

Kumar P, Yuan XH, Kumar MR, Kind R, Li XQ, et al. 2007. The rapid drift of the Indian tectonic plate. *Nature* 449:894–97

Kustowski B, Ekström G, Dziewonski AM. 2008. Anisotropic shear-wave velocity structure of the Earth's mantle: a global model. *J. Geophys. Res.* 113:B06306

Lebedev S, van der Hilst RD. 2008. Global upper-mantle tomography with the automated multimode inversion of surface and S-wave forms. *Geophys. J. Int.* 173:505–18

Lee CTA. 2003. Compositional variation of density and seismic velocities in natural peridotites at STP conditions: implications for seismic imaging of compositional heterogeneities in the upper mantle. *J. Geophys. Res.* 108(B9):2441

Lee CTA. 2006. Geochemical/petrologic constraints on the origin of cratonic mantle. In *Archean Geodynamics and Environments*, ed. K Benn, J-C Mareschal, KC Condie, *Geophys. Monogr.* 164:89–114. Washington, DC: AGU

Lee CTA, Lenardic A, Cooper CM, Niu FL, Levander A. 2005. The role of chemical boundary layers in regulating the thickness of continental and oceanic thermal boundary layers. *Earth Planet. Sci. Lett.* 230:379–95

Lehmann I. 1959. Velocities of longitudinal waves in the upper part of the Earth's mantle. *Ann. Geophys.* 15:93–118

Lehmann I. 1961. S and the structure of the upper mantle. *Geophys. J. R. Astron. Soc.* 4:124–38

Levin V, Park J. 2000. Shear zones in the Proterozoic lithosphere of the Arabian Shield and the nature of the Hales discontinuity. *Tectonophysics* 323:131–48

Li A, Burke K. 2006. Upper mantle structure of southern Africa from Rayleigh wave tomography. *J. Geophys. Res.* 111:B10303

Li C, Van Der Hilst RD, Engdahl ER, Burdick S. 2008. A new global model for *P* wave speed variations in Earth's mantle. *Geochem. Geophys. Geosyst.* 9:Q05018

Li X, Kind R, Priestley K, Sobolev SV, Tilmann F, et al. 2000. Mapping the Hawaiian plume conduit with converted seismic waves. *Nature* 405:938–41

Li X, Kind R, Yuan XH, Wolbern I, Hanka W. 2004. Rejuvenation of the lithosphere by the Hawaiian plume. *Nature* 427:827–29

Li X, Yuan X, Kind R. 2007. The lithosphere-asthenosphere boundary beneath the western United States. *Geophys. J. Int.* 170:700–10

Marone F, Gung YC, Romanowicz B. 2007. Three-dimensional radial anisotropic structure of the North American upper mantle from inversion of surface waveform data. *Geophys. J. Int.* 171:206–22

Marone F, Romanowicz B. 2007. The depth distribution of azimuthal anisotropy in the continental upper mantle. *Nature* 447:198–201

Mei S, Bai W, Hiraga T, Kohlstedt DL. 2002. Influence of melt on the creep behavior of olivine-basalt aggregates under hydrous conditions. *Earth Planet. Sci. Lett.* 201:491–507

Mercier J-P, Bostock MG, Audet P, Gaherty JB, Garnero EJ, Revenaugh J. 2008. The teleseismic signature of fossil subduction: Northwestern Canada. *J. Geophys. Res.* 113:B04308

Mierdel K, Keppler H, Smyth JR, Langenhorst F. 2007. Water solubility in aluminous orthopyroxene and the origin of the Earth's asthenosphere. *Science* 315:364–68

Mohsen A, Kind R, Sobolev SV, Weber M, the DESERT Group. 2006. Thickness of the lithosphere east of the Dead Sea Transform. *Geophys. J. Int.* 167:845–52

MONA LISA Working Group. 1997. MONA LISA—Deep seismic investigations of the lithosphere in the southeastern North Sea. *Tectonophysics* 269:1–19

Morozova EA, Morozov IB, Smithson SB, Solodilov LN. 1999. Heterogeneity of the uppermost mantle beneath Russian Eurasia from the ultra-long-range profile QUARTZ. *J. Geophys. Res.* 104(B9):20329–48

Nettles M, Dziewonski AM. 2008. Radially anisotropic shear velocity structure of the upper mantle globally and beneath North America. *J. Geophys. Res.* 113:B02303

Nishimura CE, Forsyth DW. 1989. The anisotropic structure of the upper mantle in the Pacific. *Geophys. J. Int.* 96:203–29

Oreshin S, Vinnik L, Peregoudov D, Roecker S. 2002. Lithosphere and asthenosphere of the Tien Shan imaged by S receiver functions. *Geophys. Res. Lett.* 29(8):1191

Ozacar AA, Gilbert H, Zandt G. 2008. Upper mantle discontinuity structure beneath East Anatolian Plateau (Turkey) from receiver functions. *Earth Planet. Sci. Lett.* 269:427–35

Pavlenkova GA, Priestley K, Cipar J. 2002. 2D model of the crust and uppermost mantle along rift profile, Siberian craton. *Tectonophysics* 355(1–4):171–86

Pearson DG, Carlson RW, Shirey SB, Boyd FR, Nixon PH. 1995. Stabilisation of Archean lithospheric mantle: a Re-Os isotope study of peridotite xenoliths from the Kaapvaal craton. *Earth Planet. Sci. Lett.* 134:341–57

Pedersen HA, Fishwick S, Snyder DB. 2009. A comparison of cratonic roots through consistent analysis of seismic surface waves. *Lithos* 109:81–95

Priestley K, McKenzie D. 2006. The thermal structure of the lithosphere from shear wave velocities. *Earth Planet. Sci. Lett.* 244:285–301

Revenaugh J, Jordan TH. 1991. Mantle layering from *ScS* reverberations: 3. The upper mantle. *J. Geophys. Res.* 96(B12):19781–810

Romanowicz B. 2009. The thickness of tectonic plates. *Science* 324:474–76

Roth JB, Fouch MJ, James DE, Carlson RW. 2008. Three-dimensional seismic velocity structure of the northwestern United States. *Geophys. Res. Lett.* 35:L15304

Ryberg T, Wenzel F, Mechie J, Egorkin A, Fuchs K, Solodilov L. 1996. Two-dimensional velocity structure beneath northern Eurasia derived from the super long-range seismic profile Quartz. *Bull. Seismol. Soc. Am.* 86(3):857–67

Rychert CA, Fischer KM, Rondenay S. 2005. A sharp lithosphere-asthenosphere boundary imaged beneath eastern North America. *Nature* 436:542–45

Rychert CA, Rondenay S, Fischer KM. 2007. *P*-to-*S* and *S*-to-*P* imaging of a sharp lithosphere-asthenosphere boundary beneath eastern North America. *J. Geophys. Res.* 112:B08314

Rychert CA, Shearer PM. 2009. A global view of the lithosphere-asthenosphere boundary. *Science* 324(5926):495–98

Rychert CA, Shearer PM, Fischer KM. 2010. Scattered wave imaging of the lithosphere–asthenosphere boundary. *Lithos*. In press, doi:10.1016/j.lithos.2009.12.006

Sacks IS, Snoke JA, Husebye ES. 1979. Lithosphere thickness beneath the Baltic shield. *Tectonophysics* 56:101–10

Savage B, Silver PG. 2008. Evidence for a compositional boundary within the lithospheric mantle beneath the Kalahari craton from S receiver functions. *Earth Planet. Sci. Lett.* 272:600–9

Schutt DL, Lesher CE. 2006. Effects of melt depletion on the density and seismic velocity of garnet and spinel lherzolite. *J. Geophys. Res.* 111:B05401

Sebai A, Stutzmann E, Montagner J-P, Sicilia D, Beucler E. 2006. Anisotropic structure of the African upper mantle from Rayleigh and Love wave tomography. *Phys. Earth Planet. Inter.* 155:48–62

Shapiro SS, Hager BH, Jordan TH. 1999. Stability and dynamics of the continental tectosphere. *Lithos* 48:115–33

Simons FJ, Van Der Hilst RD, Montagner J-P, Zielhuis A. 2002. Multimode Rayleigh wave inversion for heterogeneity and azimuthal anisotropy of the Australian upper mantle. *Geophys. J. Int.* 151:738–54

Sleep NH. 2005. Evolution of the continental lithosphere. *Annu. Rev. Earth Planet. Sci.* 33:369–93

Snyder DB. 2008. Stacked uppermost mantle layers within the Slave craton of NW Canada as defined by anisotropic seismic discontinuities. *Tectonics* 27:TC4006

Sodoudi F, Kind R, Hatzfeld D, Priestley K, Hanka W, et al. 2006a. Lithospheric structure of the Aegean obtained from P and S receiver functions. *J. Geophys. Res.* 111:B12307

Sodoudi F, Yuan X, Kind R, Heit B, Sadidkhouy A. 2009. Evidence for a missing crustal root and a thin lithosphere beneath the Central Alborz by receiver function studies. *Geophys. J. Int.* 177:733–42

Sodoudi F, Yuan X, Liu Q, Kind R, Chen J. 2006b. Lithospheric thickness beneath the Dabie Shan, central eastern China from *S* receiver functions. *Geophys. J. Int.* 166:1363–67

Steer DN, Knapp JH, Brown LD. 1998a. Super-deep reflection profiling: exploring the continental mantle lid. *Tectonophysics* 286:111–21

Steer DN, Knapp JH, Brown LD, Echtler HP, Brown DL, Berzin R. 1998b. Deep structure of the continental lithosphere in an unextended orogen: an explosive-source seismic reflection profile in the Urals (Urals Seismic Experiment and Integrated Studies (URSEIS 1995)). *Tectonics* 17:143–57

Stixrude L, Lithgow-Bertelloni C. 2005. Mineralogy and elasticity of the oceanic upper mantle: origin of the low-velocity zone. *J. Geophys. Res.* 110:B03204

Takei Y. 2002. Effect of pore geometry on $V_P/V_S$: from equilibrium geometry to crack. *J. Geophys. Res.* 107(B2):2043

Takei Y, Holtzman BK. 2009. Viscous constitutive relations of solid-liquid composites in terms of grain boundary contiguity: 1. Grain boundary diffusion control model. *J. Geophys. Res.* 114:B06205

Tan Y, Helmberger DV. 2007. Trans-Pacific upper mantle shear velocity structure. *J. Geophys. Res.* 112:B08301

Thybo H. 2006. The heterogeneous upper mantle low velocity zone. *Tectonophysics* 416:53–79

Thybo H, Perchuc E. 1997. The seismic 8° discontinuity and partial melting in continental mantle. *Science* 275:1626–29

van der Lee S. 2002. High-resolution estimates of lithospheric thickness from Missouri to Massachusetts, USA. *Earth Planet. Sci. Lett.* 203:15–23

van der Lee S, Nolet G. 1997. Upper mantle *S* velocity structure of North America. *J. Geophys. Res.* 102(B10):22815–38

Vinnik L, Kurnik E, Farra V. 2005. Lehmann discontinuity beneath North America: no role for seismic anisotropy. *Geophys. Res. Lett.* 32:L09306

Wittlinger G, Farra V. 2007. Converted waves reveal a thick and layered tectosphere beneath the Kalahari super-craton. *Earth Planet. Sci. Lett.* 254:404–15

Wolbern I, Jacob AWB, Blake TA, Kind R, Li X, et al. 2006. Deep origin of the Hawaiian tilted plume conduit derived from receiver functions. *Geophys. J. Int.* 166(2):767–81

Yang Y, Forsyth DW, Weeraratne DS. 2007. Seismic attenuation near the East Pacific Rise and the origin of the low-velocity zone. *Earth Planet. Sci. Lett.* 258:260–68

Yuan H, Romanowicz B. 2010. Lithospheric layering in the North American Craton. *Nature*. Submitted

Zimmerman ME, Kohlstedt DL. 2004. Rheological properties of partially molten lherzolite. *J. Petrol.* 45:275–98

Annual Review
of Earth and
Planetary Sciences

Volume 38, 2010



# Contents

**Indexes**



**Errata**

An online log of corrections to *Annual Review of Earth and Planetary Sciences* articles may be found at http://earth.annualreviews.org